

Engineered DNA Vaccination against Follicle-Stimulating Hormone Receptor Delays Ovarian Cancer Progression in Animal Models

Alfredo Perales-Puchalt,¹ Krzysztof Wojtak,¹ Elizabeth K. Duperret,¹ Xue Yang,¹ Anna M. Slager,² Jian Yan,² Kar Muthumani,¹ Luis J. Montaner,¹ and David B. Weiner¹

¹Vaccine and Immunotherapy Center, Microenvironment and Metastasis Program, The Wistar Institute, Philadelphia, PA 19104, USA; ²Inovio Pharmaceuticals, Plymouth Meeting, PA 19462, USA

Ovarian cancer presents in 80% of patients as a metastatic disease, which confers it with dismal prognosis despite surgery and chemotherapy. However, it is an immunogenic disease, and the presence of intratumoral T cells is a major prognostic factor for survival. We used a synthetic consensus (SynCon) approach to generate a novel DNA vaccine that breaks immune tolerance to follicle-stimulating hormone receptor (FSHR), present in 50% of ovarian cancers but confined to the ovary in healthy tissues. SynCon FSHR DNA vaccine generated robust CD8⁺ and CD4⁺ cellular immune responses and FSHR-redirected antibodies. The SynCon FSHR DNA vaccine delayed the progression of a highly aggressive ovarian cancer model with peritoneal carcinomatosis in immunocompetent mice, and it increased the infiltration of anti-tumor CD8⁺ T cells in the tumor microenvironment. Anti-tumor activity of this FSHR vaccine was confirmed in a syngeneic murine FSHR-expressing prostate cancer model. Furthermore, adoptive transfer of vaccine-primed CD8⁺ T cells after *ex vivo* expansion delayed ovarian cancer progression. In conclusion, the SynCon FSHR vaccine was able to break immune tolerance and elicit an effective anti-tumor response associated with an increase in tumor-infiltrating T cells. FSHR DNA vaccination could help current ovarian cancer therapy after first-line treatment of FSHR⁺ tumors to prevent tumor recurrence.

INTRODUCTION

Ovarian cancer is the fifth leading cause of cancer-related death in women, with around 22,000 new cases diagnosed per year in the United States.¹ Despite important advances in surgery (as complete cytoreduction)² and chemotherapy, there is still ample room for improvement in the prognosis of this disease. Ovarian cancer has been found to be an immunogenic disease. The presence of intratumoral T cell infiltration, in particular of CD8 T cells, has been reported to correlate with disease-free and overall survival.^{3,4} Therefore, immunotherapies have the potential to reverse the dismal prognosis.⁵

The follicle-stimulating hormone receptor (FSHR) is a transmembrane tumor-associated antigen expressed in about 50% of ovarian tumors of different histological type and not expressed in extragonadal

tissues. Expression of FSHR has also been reported in the endothelial cells of microvasculature of about 70% of tumors, but not in not-cancer-related neoangiogenesis,⁶ and in the endothelium of 79% of metastasis irrespective of the FSHR expression in the primary tumor.⁷ Additionally, FSHR overexpression has been reported in 70% of prostate cancer.⁸ We recently helped to establish that FSHR is an optimal target for the treatment of ovarian cancer, and we proved the safety of targeting FSHR in an immunocompetent mouse, showing, as predicted, no adverse effects.⁹

Given the immunotherapeutic potential of FSHR, we chose to target it using a DNA vaccination. Newer designed and optimized DNA vaccines have recently shown strong CD8 and CD4 T cell responses in clinical trials.^{10–13} These new DNA vaccines, unlike peptide vaccines, are not human leukocyte antigen (HLA) restricted and can be robustly presented on major histocompatibility complex (MHC) class I and MHC class II, and they can be designed to drive class II responses and break immune tolerance.^{14,15} In synthetic consensus (SynCon) DNA vaccines, sequences are compared across species to identify a consensus sequence with approximately 95% homology to the native sequence. We have shown that SynCon DNA vaccines elicit immune responses that allow for class II help, due to the generation of neoantigens to which there is no central tolerance. SynCon vaccines can drive anti-tumor responses that delay tumor progression, targeting self-antigens more efficiently than vaccinating with native antigens.^{16,17} We have also shown in a phase II clinical trial that we can revert cervical intraepithelial neoplasia with a consensus vaccine targeting HPV.¹⁸

In this paper, we describe the study of optimized DNA vaccines encoding the native or a SynCon sequence for murine FSHR. We show that vaccination with the SynCon immunogen can break

Received 14 August 2018; accepted 13 November 2018;
<https://doi.org/10.1016/j.ymthe.2018.11.014>

Correspondence: David B. Weiner, PhD, Vaccine and Immunotherapy Center, Microenvironment and Metastasis Program, The Wistar Institute, 3601 Spruce Street, Philadelphia, PA 19104, USA.

E-mail: dweiner@wistar.org

immunological tolerance to FSHR and generates potent CD8⁺ and CD4⁺ responses against the FSHR more efficiently than the native immunogen. To determine the anti-tumor activity of the FSHR SynCon vaccine, we used a preclinical model of aggressive peritoneal carcinomatosis in which syngeneic epithelial ovarian tumor cells (ID8-Defb29/Vegf-a) develop intraperitoneal tumors and ascites that recapitulate the inflammatory microenvironment of human ovarian tumors.^{19–21} In it, we show that vaccination with the FSHR SynCon vaccine delayed ovarian cancer progression through a CD8-dependent mechanism.

RESULTS

Design of the Mouse FSHR Vaccine

Two vaccines against murine FSHR (Uniprot: P35378) were generated using either the native or a SynCon FSHR sequence. The murine SynCon FSHR was constructed by generating a consensus FSHR sequence using sequences from mouse and lower animals. Additionally, one mutation to disrupt hormone binding and two mutations to disrupt G-protein activation were introduced. The resulting SynCon murine FSHR sequence shares 95.7% homology with native murine FSHR. A native murine FSHR vaccine was generated using the native murine FSHR sequence.

To have a higher level of expression, the native leader sequence was removed from both the native and SynCon antigens, and an upstream Kozak sequence and immunoglobulin E (IgE) leader sequence were added to the N terminus²² (Figure 1A). Codon and RNA optimization was performed, and the final optimized genes were each subcloned into a modified pVAX1 expression vector (Figure 1B). Expression of these DNA-encoded FSHR vaccines was detected by immunofluorescence and western blot in transduced 293T cells (Figure 1C; Figure S1B). The lower signal detected in the FSHR SynCon 293T cells could be due to a lower number of B cell epitopes in SynCon due to the sequence changes, as sera from native FSHR-immunized mice was used for staining.

Mouse FSHR DNA Vaccines Generate Durable and Robust Cellular and Humoral Responses

To determine the ability to break immunological tolerance and immunostimulatory capacity of our mouse FSHR DNA vaccines, we immunized mice with 3 doses of FSHR DNA vaccines (native or SynCon) or empty vector by using electroporation, as previously described.¹⁶ We administered vaccinations in 2-week intervals, and we sacrificed the mice a week after the last immunization (Figure 2A). Both vaccines showed strong cellular responses, as measured by interferon- γ (IFN γ) enzyme-linked immunospot (ELISPOT), when pulsed with 15-mers from the SynCon vaccine-matched protein or from the native murine FSHR (Figures 2B and 2C). To determine if a specific part of the vaccine was more immunogenic, we separated the stimulating peptides into 3 independent peptide pools. We observed that the T cell IFN γ responses were evenly distributed along the 3 parts of the protein, but the SynCon vaccine was able to increase the responses against the central part of the FSHR (Figures 2C and 2D). In all cases, the SynCon FSHR vaccine showed higher re-

sponses than the native vaccine, suggesting a better ability to break tolerance acquired by its higher degree of diversity from the original sequence (Figures 2B–2D).

To determine the source of the cellular responses, we harvested the splenocytes from the vaccinated mice, and we stimulated them with FSHR-derived overlapping 15-mers for flow cytometric analysis. We found that both CD4⁺ and CD8⁺ T cells were being stimulated by the mouse FSHR vaccine (Figure 3; Figure S2). CD4⁺ and CD8⁺ T cells derived from the SynCon FSHR vaccine resulted in a significantly higher expression of IFN γ , tumor necrosis factor alpha (TNF- α), and interleukin-2 (IL-2) when compared to the empty vector-treated group (Figures 3A and 3C). Both FSHR vaccines showed an increase in the generation of polyfunctional T cells that were able to produce all three cytokines (Figure 3B). The CD4⁺ T cell responses elicited by our FSHR vaccines were significantly higher than those in the control group, with the FSHR SynCon vaccine eliciting the highest responses (Figure 3C). Both vaccines were also able to generate a high number of polyfunctional CD4⁺ T cells against FSHR (Figure 3D) but at different magnitudes.

FSHR is a tumor-associated antigen that has the advantage of being a transmembrane protein. This allows the immune targeting of this protein not only through cellular T cell responses but also through antibody responses. To study if our vaccine could also elicit a humoral response against FSHR, we analyzed serum from our vaccinated mice for anti-FSHR antibodies. To do that, we performed a binding ELISA using the extracellular domain of FSHR. We found 3 immunizations were able to establish anti-FSHR antibodies in the majority of the mice (Figure S3).

Murine FSHR DNA Vaccines Generate a Long-Lasting Cellular Response

The durability of vaccine responses is important for the prevention of primary tumor development as well as recurrence. To test the ability of our FSHR vaccine to generate immune memory, we immunized mice with 3 doses of FSHR native or SynCon vaccines or empty vector, and we measured responses 3 months after vaccination (Figure 4A). A significant immune response was present at 3 months, as measured by IFN γ ELISPOT against the FSHR-derived peptides (Figures 4B and 4C). The frequencies of CD8⁺ and CD4⁺ T cells able to secrete IFN γ , TNF α , and IL-2 to peptides derived from FSHR native protein were similar to the week after the last immunization. As noted before, SynCon FSHR vaccine responses were higher than native FSHR (Figures 4D–4I).

As the SynCon FSHR vaccine showed superior immunogenicity compared to the native FSHR vaccine, we opted to continue further study of the SynCon FSHR vaccine.

Mouse FSHR SynCon DNA Vaccine Delays Growth of FSHR⁺ Ovarian Tumors

We recently reported that FSHR is expressed in approximately 50% of ovarian cancers.⁹ After the first-line therapy of debulking surgery and

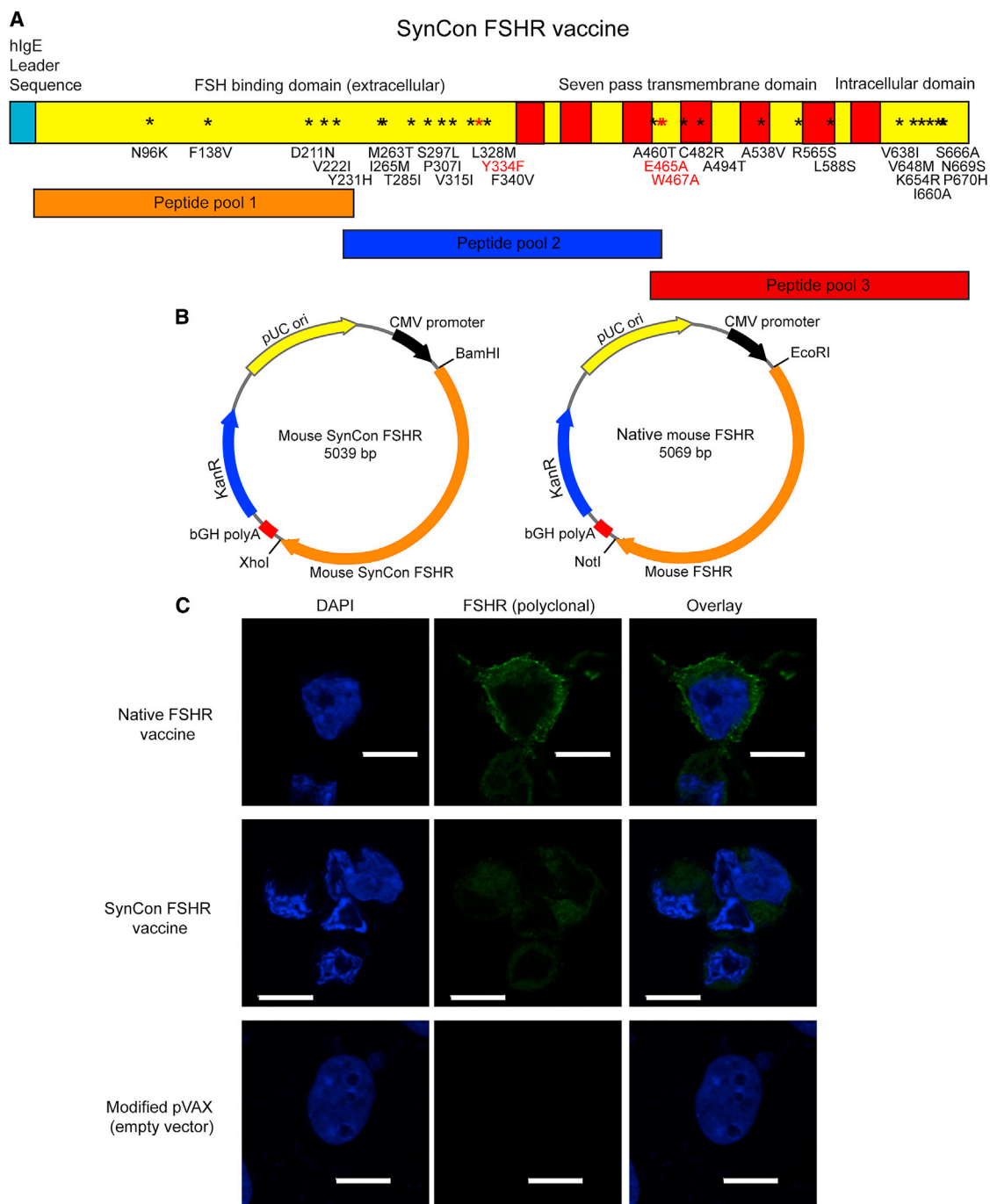


Figure 1. Design and Expression of Murine FSHR Native and SynCon Vaccines

(A) Depiction of murine FSHR native and consensus vaccines and stretches encompassed by the peptide pools. Mutations for FSHR-signaling ablation are depicted in red, and mutations for the SynCon sequence are depicted in black. (B) Schematic subcloning strategy into modified pVAX. (C) Immunofluorescence of 293T cells transfected with murine FSHR consensus vaccine, murine native FSHR vaccine, or modified pVAX empty vector stained with polyclonal anti-mouse FSHR antibody (representative of 2 independent experiments). *Mutation. Scale bars, 10 μ m.

chemotherapy, 75% of ovarian cancer patients are disease-free for at least 12 months, after which ovarian cancer recurs. We wanted to study the ability of the mouse FSHR SynCon vaccine to prevent

recurrent disease in FSHR-expressing tumors. We vaccinated groups of mice with either FSHR SynCon vaccine or empty vector (Figure 5A). A week after the third immunization, we challenged these

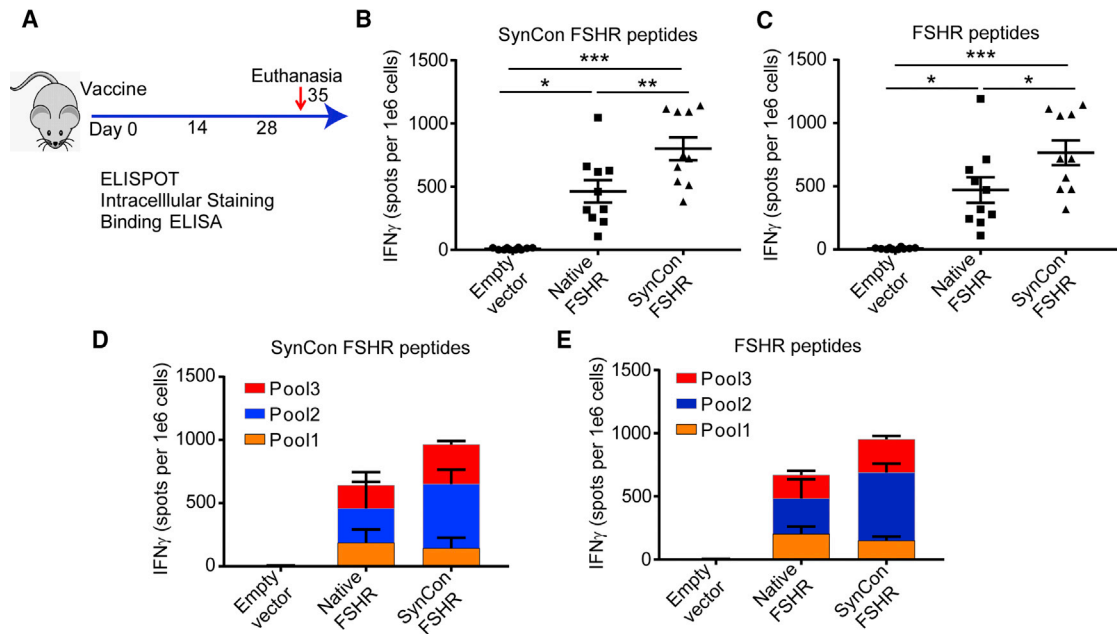


Figure 2. Murine FSHR SynCon Vaccine Generates Robust Interferon Gamma Responses

(A) Schematic of immunization protocol. (B–E) IFN γ ELISPOT of splenocytes from mice immunized with murine FSHR SynCon vaccine, native FSHR vaccine, or empty vector pulsed with (B and D) SynCon vaccine-matched or (C and E) FSHR-derived peptides, shown as total spots per mouse or aggregated per peptide pool (pooled from 2 independent experiments of $n = 5$ mice). ANOVA. Error bars represent SEM. * $p < 0.05$, ** $p < 0.01$, *** $p < 0.001$.

immunocompetent mice with the syngeneic, highly aggressive ovarian cancer cell line ID8-*Defb29/Vegf-a-Fshr*.⁹ This cell line mimics a late-stage ovarian tumor, developing as peritoneal carcinomatosis with multiple microscopic peritoneal nodules and a rapid accumulation of ascites.

The SynCon FSHR vaccine delayed tumor progression in this ovarian cancer model, increasing survival by 3-fold in 25% of the mice (Figure 5B). Using a luciferase system, we measured tumor burden during the experiments, showing a significant decrease in tumor burden in the mice treated with the FSHR SynCon vaccine (Figures 5C and 5D; Figure S4A). An increase in T cell responses against the tumor was detected in the peritoneal wash in vaccinated mice 3 weeks after tumor inoculation (Figure 5E). This increased T cell compartment in the tumor microenvironment presented a higher proportion of CD8⁺ T cells (Figures 5F and 5G). To ensure the anti-tumor specificity of this T cell-enriched microenvironment, we then performed IFN γ ELISPOTs using the tumor microenvironment-derived cells obtained by paracentesis, pulsing them with native FSHR peptides. Results showed a reproducible IFN γ response from the tumor microenvironment of FSHR-vaccinated mice, but not from the control pVAX groups (Figure 5H), suggesting that the normal expression of FSHR in the tumor cells was not able to break immune tolerance by itself.

Validation of FSHR as a Target Antigen for Tumor Regression in Prostate Cancer

To test if the FSHR SynCon vaccine would also be useful in the treatment of other tumor types, we chose the murine prostate cancer

model TRAMPC2. As FSHR is expressed in 70% of prostate cancers,⁸ we expressed murine FSHR in this cell line to recapitulate the FSHR⁺ prostate tumors. We then vaccinated a cohort of 10 male mice with the FSHR vaccine or the empty vector, and, a week after the third vaccination, we inoculated 2,000,000 TRAMPC2-Fshr cells into their flank. We then followed tumor progression, and we found that the murine FSHR SynCon vaccine also delayed tumor progression in this solid tumor model (Figure 5I).

Importantly, we observed that the immune pressure elicited by the FSHR SynCon DNA vaccine significantly delayed tumor progression of different FSHR⁺ tumor models, doing so by increasing the compartment of FSHR-specific anti-tumor T cells that were being recruited into the tumor microenvironment.

Vaccine-Primed Anti-FSHR CD8⁺ T Cells Are Necessary for the Effect of the SynCon FSHR Vaccine

Effector CD8⁺ T cells are considered the main actors in the anti-tumor immune response.^{2,3} As shown above, the FSHR SynCon vaccine is able to induce potent anti-FSHR CD8⁺ T cells. We intended to determine the role of the newly generated CD8⁺ T cells in the observed anti-tumor effect of the vaccine. To do so, immunized cohorts of mice with FSHR SynCon vaccine or empty vector were treated with anti-CD8 or irrelevant immunoglobulin G (IgG), starting 3 days before tumor challenge and then twice weekly until the end of the experiment. We challenged the mice with ID8-*Defb29/Vegf-a-Fshr* a week after the final immunization and followed survival (Figure 6A; Figure S4B). The survival

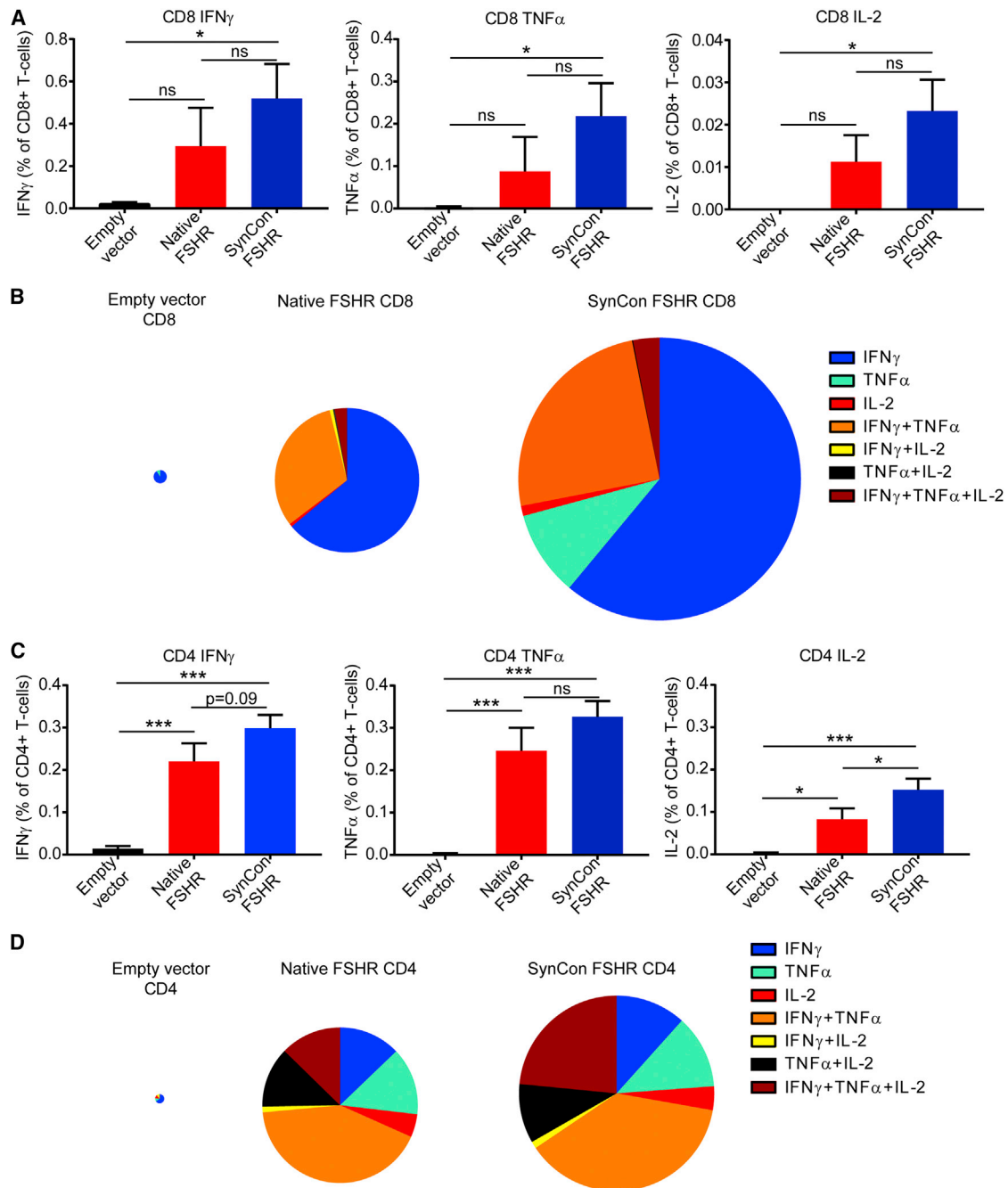


Figure 3. Murine FSHR SynCon Vaccine Generates Strong CD8 and CD4 Responses

(A and C) Percentages of IFN γ , TNF- α , and IL-2 produced by (A) CD8 $^{+}$ or (C) CD4 $^{+}$ T cells from the spleen of mice immunized with murine FSHR SynCon vaccine, murine native FSHR, or pVAX stimulated with native murine FSHR peptides. (B and D) Pie charts representing the cytokines produced by (B) CD8 and (D) CD4 T cells of each of the groups. The pie size corresponds to the number of responding T cells ($n = 5$ mice per group). ANOVA. Error bars represent SEM. * $p < 0.05$, ** $p < 0.01$, *** $p < 0.001$.

benefit generated by the vaccine was completely abrogated in the absence of CD8 $^{+}$ T cells, suggesting the importance of CD8 $^{+}$ -mediated immunity in the anti-tumor FSHR vaccine response (Figure 6B).

To study the *in vivo* anti-tumor relevance of the CD4 responses elicited by the FSHR SynCon vaccine, we similarly depleted CD4 T cells after immunization starting 3 days before tumor challenge. Depletion of CD4 T cells also resulted in a loss in vaccine-induced

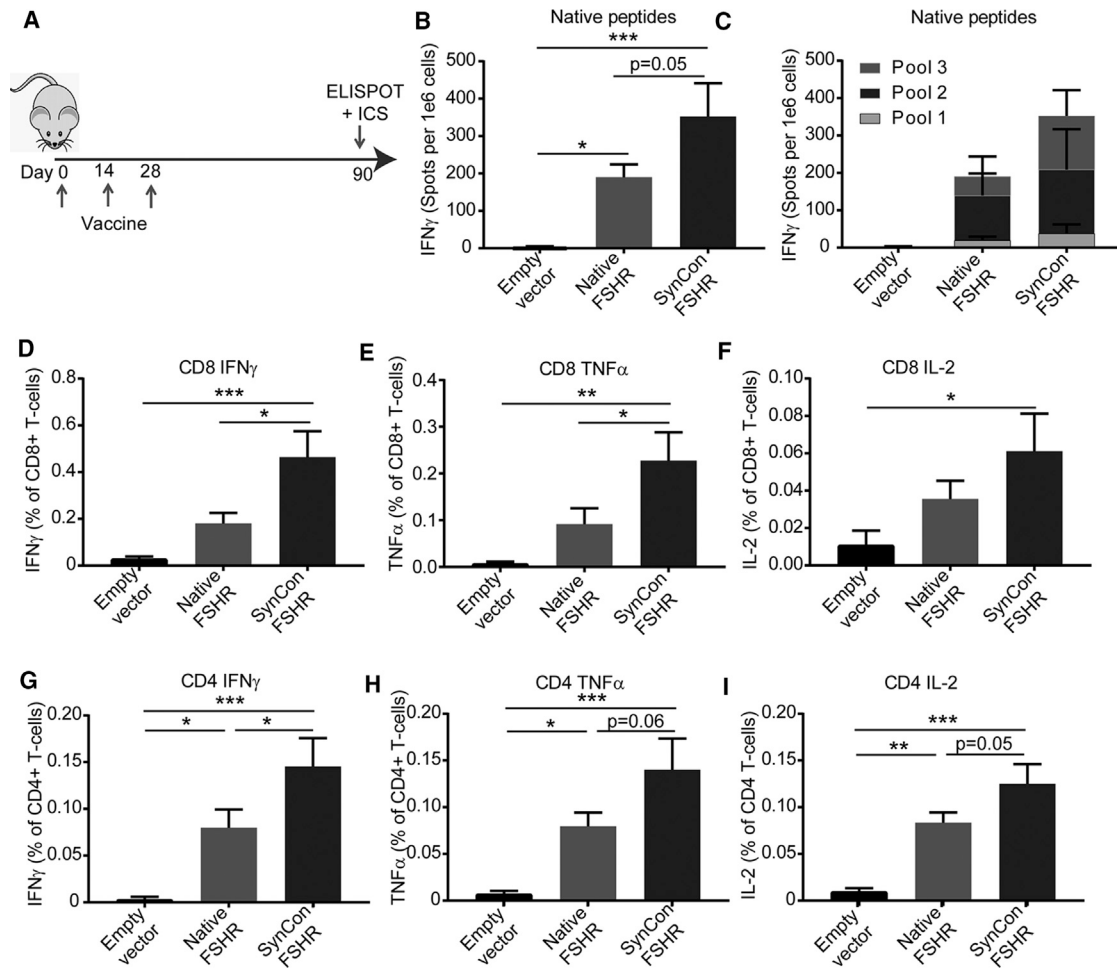


Figure 4. Murine FSHR SynCon Vaccine Generates a Long-Lasting Cellular Response

(A) Schematic of immunization protocol. IFN γ ELISPOT of splenocytes from mice immunized with murine FSHR SynCon vaccine, native FSHR vaccine, or empty vector pulsed with FSHR-derived peptides is shown as (B) total spots or (C) aggregated per peptide pool. (D–I) Percentages of (D and G) IFN γ , (E and H) TNF- α , and (F and I) IL-2 produced by CD8 $^{+}$ and CD4 $^{+}$ T cells from the spleen of mice immunized with mouse FSHR SynCon vaccine, native FSHR vaccine, or empty vector, stimulated with murine FSHR-derived peptides. (Pool of 2 independent experiments with a total of $n = 7$ –9 mice per group.) ANOVA. Error bars represent SEM. * $p < 0.05$, ** $p < 0.01$, *** $p < 0.001$.

survival. However, CD4-depleted vaccinated mice survived significantly longer than the controls (Figure S4C). This shows that, despite CD4 depletion, the vaccine still had some efficacy, supporting the important role of the CD8 T cells.

FSHR Epitope STYRLKKL Identified as Immunodominant in the FSHR-Specific Vaccine Response

To determine what epitope may mediate the CD8 $^{+}$ T cell response following vaccination, we harvested the spleens from vaccinated mice, and we performed ELISPOT assays using a peptide library encoding for the 10 peptides predicted to have the highest affinity in the MHC class I binding prediction program from the immunopeptide database (<http://tools.iedb.org/mhci/>). We found that the FSHR SynCon vaccine elicited stronger responses than the native FSHR vaccine, with T cells consistently recognizing more epitopes (Figure 6C; Figures S5A and S5B).

We expanded the responding FSHR T cells until we obtained enriched populations of FSHR-peptide-specific CD8 $^{+}$ clones, which responded in a dose-dependent manner after being activated with different doses of peptide (Figure 6D; Figure S5C). We found that the T cell clones that were being stimulated with the 15-mer that encoded for the peptide STYRLKKL were able to respond to doses of peptide as low as 0.01 $\mu\text{g}/\text{mL}$ (Figure 6D; Figure S5C). STYRLKKL is an octamer predicted to bind to murine MHC-I H2-K(b) molecule with an affinity of 33 nM, and it has a high score for proteasome degradation and TAP binding (<http://tools.iedb.org/processing/>; Figure S6). To verify the presence of STYRLKKL-specific T cells *in vivo* after vaccination, we generated a PE-labeled tetramer through the NIH Tetramer Core, and we determined the percentage of T cells that were able to bind to this MHC-peptide complex. We found a significant number of STYRLKKL $^{+}$ CD8 $^{+}$ T cells still circulating in peripheral blood 3 months after vaccination in naive mice (Figure 6E).

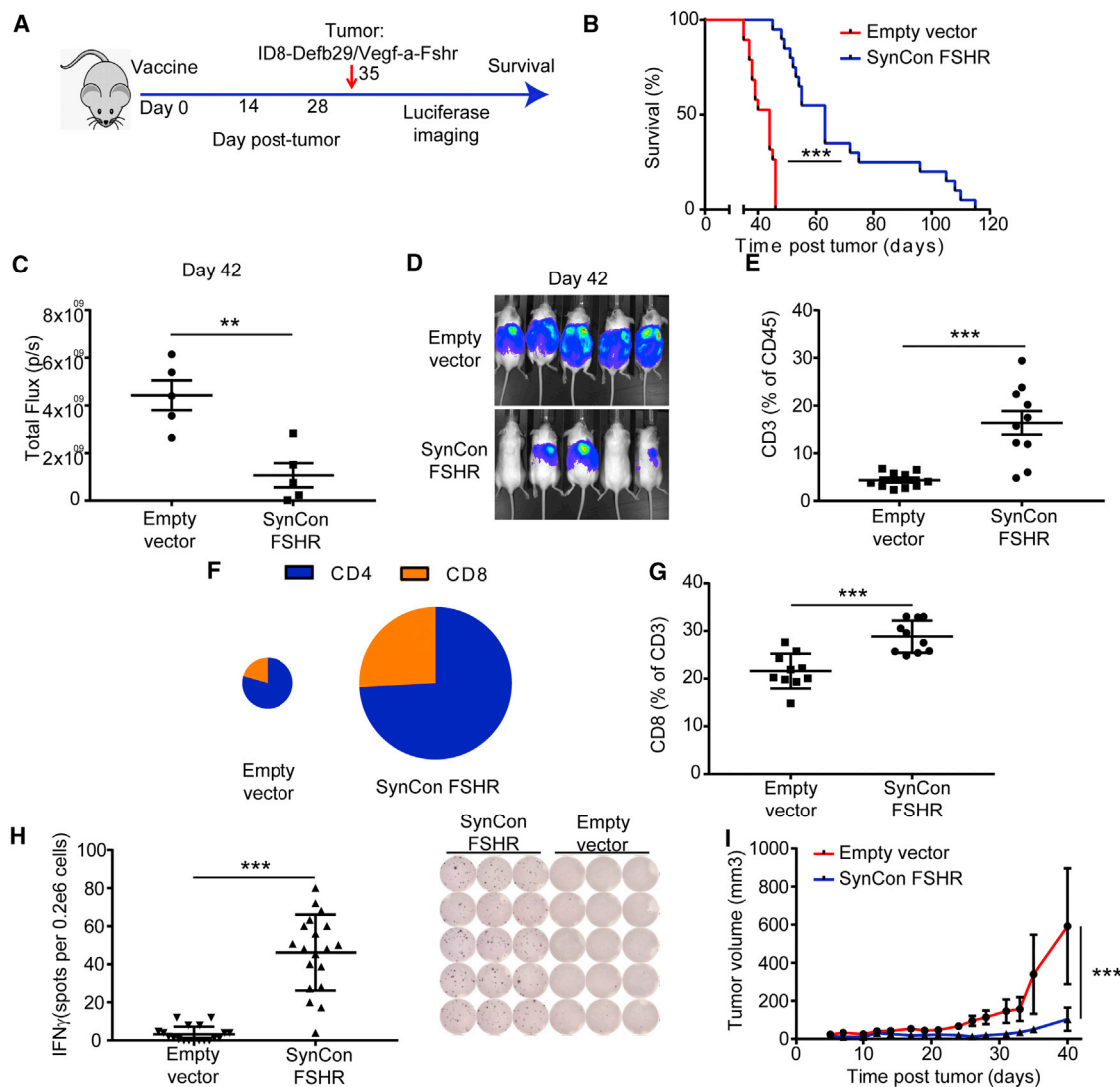


Figure 5. Murine FSHR SynCon Vaccine Delays Growth of FSHR⁺ Tumors and Promotes Recruitment of T Cells to the Tumor Microenvironment

(A) Schematic of tumor challenge experiments. (B) Survival curve of ID8-Defb29/Vegf-a-Fshr-bearing mice treated with murine FSHR SynCon vaccine or pVAX empty vector (pooled from 3 independent experiments of $n = 5$ –10 mice per group). (C and D) Luciferase quantification (C) and image (D) of ID8-Defb29/Vegf-a-Fshr-bearing mice treated with mouse FSHR vaccine or empty vector on day 42 of tumor progression (representative of 2 independent experiments of $n = 5$ mice per group). (E) Percentage of T cells of the total CD45⁺ cells in the tumor microenvironment ($n = 10$, pool of 2 independent experiments). (F) Pie charts representing the proportion of CD4⁺ and CD8⁺ T cells in the tumor microenvironment of each of the groups. The pie size corresponds to the percentage of total T cells in the tumor microenvironment. (G) Percentage of CD8⁺ T cells of the total T cells in the tumor microenvironment of mice from the different groups ($n = 10$, pool of 2 independent experiments). (H) Interferon- γ ELISPOT of cells from the tumor microenvironment from mice treated with murine FSHR SynCon vaccine or empty vector pulsed with murine FSHR peptides and ELISPOT representative picture (pool of 3 independent experiments with $n = 5$ –10 mice per group). (I) Tumor volume of mice bearing TRAMP2-Fshr treated with mouse FSHR vaccine or empty vector (log rank, unpaired t test, and linear regression). Error bars represent SEM. ** $p < 0.01$, *** $p < 0.001$.

FSHR_{STYRLKKL}-Specific CD8⁺ T Cells from 3 Months after Vaccination Are Cytotoxic against Tumor and Can Delay Tumor Progression upon Adoptive Transfer

Next, we sought to determine if the FSHR-specific T cells that we had been able to isolate 3 months after vaccinating mice were able to kill specifically FSHR⁺ tumor cells. We co-cultured either ID8-Defb29/Vegf-a or ID8-Defb29/Vegf-a-Fshr cells with FSHR_{STYRLKKL}-specific

T cells from mice vaccinated 3 months earlier. We found that these T cells were able to kill FSHR⁺ tumor cells very efficiently, and they did not kill the non-FSHR-expressing cells (Figure 6F). We then determined the *in vivo* anti-tumor effect of these anti-FSHR T cells. To do so, we challenged naive mice with ID8-Defb29/Vegf-a-Fshr, and, 24 hr later, we injected 2 million FSHR-specific or non-specifically (anti-CD3 anti-CD28) expanded T cells or vehicle (PBS). We

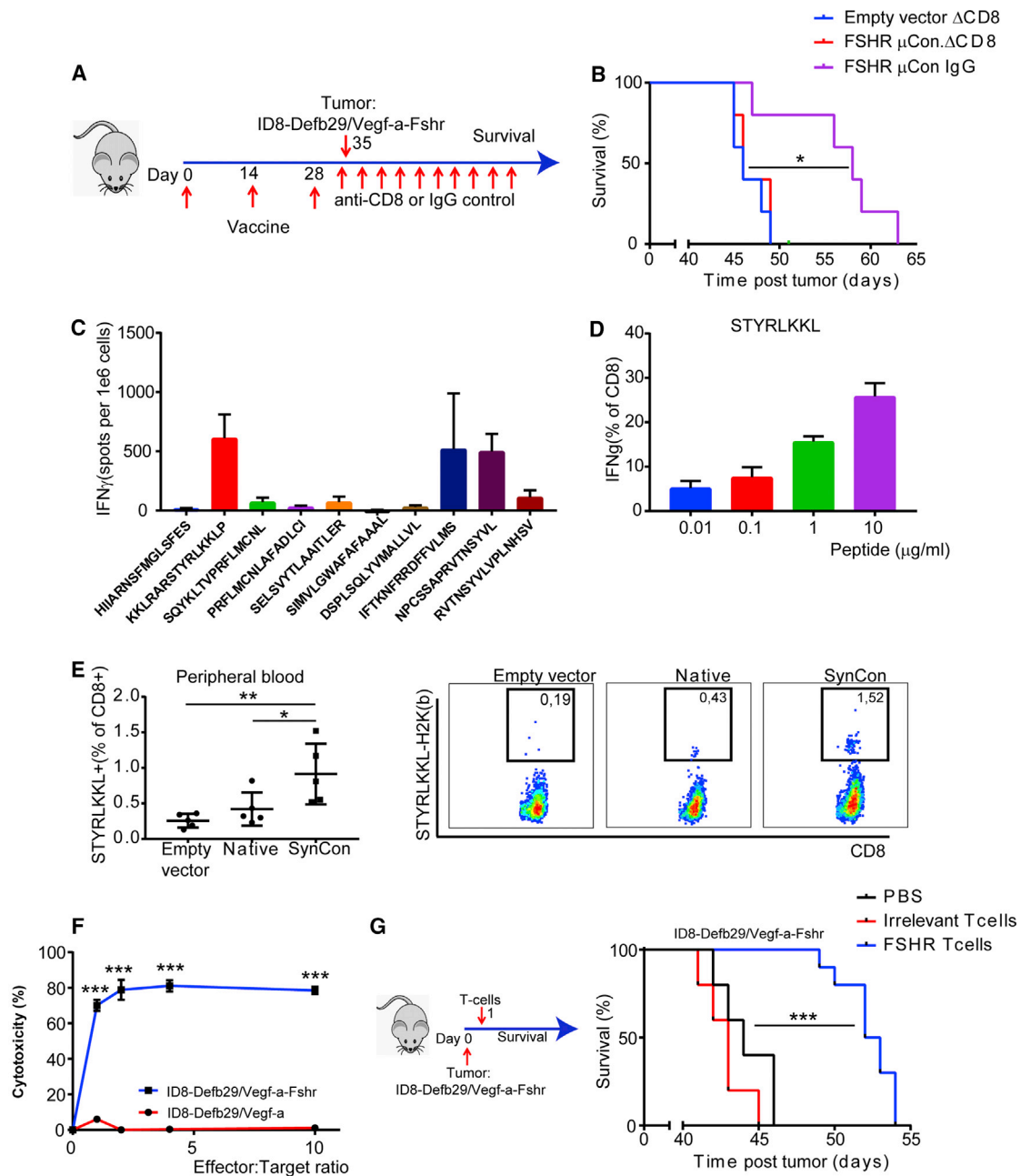


Figure 6. Vaccine-Primed Anti-FSHR CD8⁺ T Cells Are Necessary for the Effect of the FSHR SynCon Vaccine and Able to Delay FSHR⁺ Tumor Progression
 (A) Schematic of tumor challenge depletion experiment: we vaccinated mice and challenged with ID8-Defb29/Vegf-a-Fshr 1 week after the last immunization. At 1 day prior to the tumor challenge and twice weekly thereafter, we administered either anti-mouse CD8 or rat polyclonal IgG. (B) Survival plot of the FSHR SynCon vaccine or pVAX empty vector with or without CD8 depletion (single experiment with n = 5 mice per group). (C) Interferon- γ ELISPOT of splenocytes from mice treated with murine FSHR consensus vaccine pulsed with murine FSHR peptides (one experiment with n = 4 mice). (D) Percentage of CD8⁺ T cells producing IFN γ upon stimulation with STYRLKKL peptides at different concentrations (representative of 2 independent experiments). The T cells of this experiment were expanded with KKLRLARSTYRLKKLP peptide except for those in the last column, which were expanded with IFTKNFRDRDFVILMS. (E) Histogram and representative flow cytometry plots of H2-K(b)-STYRLKKL tetramer CD8⁺ T cells in peripheral blood of mice vaccinated with FSHR consensus vaccine, native vaccine, or pVAX 90 days after first vaccination. (F) Cytotoxicity of T cells derived from murine FSHR SynCon vaccine expanded with KKLRLARSTYRLKKLP peptide (5 ng/mL) 4 weeks after starting peptide stimulation of ID8-Defb29/Vegf-a or ID8-Defb29/Vegf-a-Fshr tumor cells, measured by 7-AAD/Annexin V flow cytometric staining after co-culture of 5 hr (representative of 2 independent experiments). (G) Survival plot of mice challenged with 2 million ID8-Defb29/Vegf-a-Fshr cells and treated a day later with 2 million FSHR_{STYRLKKL}-specific T cells expanded *ex vivo* (n = 10 mice), anti-mouse CD3/CD28 bead-expanded T cells (n = 5 mice), or vehicle (PBS; n = 5 mice) (log rank, one-way ANOVA, and unpaired t test). Error bars represent SEM. *p < 0.05, **p < 0.01, ***p < 0.001.

found that the FSHR_{STYRLKKL}-specific T cells were able to significantly delay tumor progression (Figure 6G).

Together, we observed that the SynCon vaccine-primed anti-FSHR CD8⁺ T cells, which were required for the effect of the FSHR consensus vaccine, and these specific CD8⁺ T cells are able to prolong survival in an FSHR⁺ tumor.

DISCUSSION

In this paper, we describe for the first time the generation of a vaccine against FSHR. This designed synthetic SynCon DNA vaccine targeting FSHR was able to break immune tolerance, elicit potent CD8⁺ and CD4⁺ long-lasting responses, and delay FSHR⁺ tumor progression by enhancing anti-tumor immunity, specifically CD8⁺ cytotoxic T lymphocyte (CTL) responses.

FSHR is expressed in approximately 50% of ovarian cancers⁹ and in endothelial cells of the microvasculature of about 70% of tumors⁶ and 79% of metastasis (irrespective of the FSHR expression in the primary tumor).⁷ In healthy tissues, we only found FSHR to be expressed on the ovaries in females, and its levels cycle, reaching high levels only in the granulosa cells of the selected follicle. As the ovaries are removed at the time of surgical debulking, which is typically the first step in the treatment of ovarian cancer, no adverse effects should be expected from targeting FSHR. Even in the case of irresectable disease, due to the selective expression of FSHR, we would not expect significant adverse effects other than infertility. The safety of these approaches also has been supported by the lack of adverse effects seen after targeting the FSHR using FSHR-redirectioned T cells^{9,24} and our experience with the FSHR vaccine.

The use of DNA vaccination for cancer provides multiple advantages over other vaccination strategies. The expression of the full protein allows a T cell priming that is not restricted to certain HLA (typically A2) molecules, as is the case for peptide-based vaccines.^{25,26} DNA vaccination additionally promotes the generation of both CD8⁺ and CD4⁺ T cells through direct intracellular synthesis of protein for presentation on MHC class I and class II.²⁷ Dendritic cell vaccines have also shown promise in ovarian cancer; however, they require the presence of a tumor to pulse dendritic cells, which prevents their use in a prophylactic setting, and they require a more complex and personalized development.^{28,29}

The presence of intratumoral T cells, in particular of CD8 T cells, has been reported to correlate with disease-free and overall survival.^{3,4} Mechanistically, priming of cytotoxic CD8 T cells against certain tumor antigens allows CD8 T cell detection and killing of the tumor cells.²³ However, ovarian and other cancers have multiple mechanisms of immune evasion, such as the recruitment of immunosuppressive cell types (T regs or suppressive myeloid cells) and secretion of immunomodulatory proteins (transforming growth factor β [TGF- β], IL-10, etc.).^{30,31} In this paper, we report that a SynCon electroporation-delivered DNA vaccine against FSHR is able to generate FSHR-specific T cells and to increase the presence of T cells in the

tumor microenvironment, resulting in increasing the survival of ovarian cancer-bearing mice. This approach would be of great interest in the treatment of ovarian cancer. After the first-line therapy of debulking surgery and chemotherapy, 75% of ovarian cancer patients are disease-free for at least 12 months, after which ovarian cancer recurs, limiting the therapeutic options.³² Currently, there is a great need to develop therapies that can help prolong this maintenance setting after competition of first-line or recurrent ovarian cancer treatment. Similar to recent clinical results with PARP inhibitors in the case of BRCA-mutated tumors,^{33–35} an FSHR vaccine would potentially be of great value in patients with FSHR-positive ovarian cancers. With vaccine administration following chemotherapy, at a stage of minimal residual disease, the increased immune pressure could impact the recurrence of ovarian cancer in the presence of a more favorable immune environment.

The cytolytic effect of CD8⁺ T cells is a paradigm of anti-tumor immunity.²³ More recently engineered DNA vaccines delivered by CELLECTRA electroporation have shown in clinical trials a unique ability to generate CD8⁺ T cells both in cancer^{10,18} and infectious disease^{11,36} settings. The ability of the FSHR DNA vaccine to break immunological tolerance allowed the priming and expansion of CD8⁺ T cells that can respond against FSHR-bearing tumors. Here we show that the anti-FSHR T cells could specifically kill FSHR⁺ ovarian cell lines *in vitro* and delay FSHR⁺ ovarian and prostate cancer progression *in vivo*. These findings could potentially be used to boost the anti-tumor effect of the vaccine by using adoptive cell transfer. Following vaccination, newly created *in vivo* primed CD8⁺ T cells could be extracted from patients by leukapheresis and further expanded *ex vivo* with FSHR-derived peptides for possible reintroduction. The benefits of such expansion *in vitro* to continued expansion *in vivo* by vaccination could be compared.

In conclusion, an engineered SynCon DNA vaccine targeting FSHR breaks tolerance and can generate robust and long-lasting anti-FSHR immunity. This approach can be used as an important and likely safe approach for the treatment and prevention of ovarian cancer and multiple other FSHR-expressing tumors.

MATERIALS AND METHODS

Animals and Cell Lines

C57BL/6 and B6(Cg)-Tyr^{c-2j}/J mice were purchased from Jackson ImmunoResearch Laboratories. Animal experiments were approved by the Institutional Animal Care and Use Committee at the Wistar Institute.

ID8-*Defb29/Vegf-a-Fshr* cells express similar levels of FSHR as OVCAR3 human ovarian cancer (Figure S1A), and they were provided by J.R. Conejo-Garcia (Department of Immunology, Moffitt Cancer Center, FL). We generated intraperitoneal tumors using ID8-*Defb29/Vegf-a-Fshr* by injecting 2 million cells intraperitoneally, and survival was monitored as described previously.⁹ TRAMP-C2 cells were purchased from ATCC and retrovirally transduced to express murine FSHR. We generated subcutaneous tumors by injecting

2 million cells in the axillary flank. Experiments were started when mice were between 6 and 8 weeks. ID8-*Defb29/Vegf-a-Fshr* cells were injected into female mice and TRAMP-C2 cells into male mice. 293T cells were purchased from ATCC.

Mice were treated by injecting 25 µg DNA resuspended in 30 µL water into the tibialis anterior muscle followed by electroporation with the CELLECTRA device (Inovio Pharmaceuticals).

Design of FSHR Vaccine

Murine SynCon FSHR DNA vaccine was designed by using a SynCon technology. Briefly, a sequence that shares 95.7% homology with murine FSHR was generated by using FSHR sequences from mouse and other animal sequences to obtain a phylogenetically conserved sequence that shared approximately 95% homology with mouse. Mutations were introduced to ablate function.^{16,17} A native murine FSHR was also generated. The native FSHR leader sequence was replaced from both the SynCon and native sequences with an IgE leader sequence. Codon and RNA optimization was performed, and the final optimized genes were each subcloned into a modified pVAX1 expression vector ([Supplemental Materials and Methods](#)).

In Vivo Antibody Treatment

200 µg anti-mouse CD8 (YTS169.4), anti-mouse CD4 (GK1.5), or polyclonal rat IgG was administered intraperitoneally 4 days before tumor inoculation and twice a week until the end of the experiment.

Flow Cytometry

We used a BD LSRII flow cytometer or BD FACSAria cell sorter (BD Biosciences).

Anti-mouse antibodies used were directly fluorochrome conjugated. We used CD3e (17A2), CD4 (RM4-5), CD8b (YTS156.7.7), CD45 (30-F11), IFN γ (XMG1.2), TNF- α (MP6-XT22), and IL-2 (JES6-5H4), all from BioLegend. Live-dead exclusion was done with Violet viability kit (Invitrogen).

For the determination of intracellular cytokines, we cultured 2 million splenocytes in the presence of peptides derived from murine native or SynCon FSHR for 4–5 hours in the presence of Golgi-stop protein transport inhibitor (BD Biosciences), followed by surface and intracellular staining.

We obtained the phycoerythrin (PE)-labeled STYRLKKL-H2K(b) from the NIH Tetramer Core.

ELISPOT

We harvested splenocytes and coincubated them with FSHR peptide pools from native or the consensus isoforms of FSHR for 24 hr. We performed the mouse IFN γ ELISPOT according to the manufacturer's instructions (Mabtech).

To test immunogenicity, we generated 15-mers overlapping by 9 amino acids encompassing the whole FSHR proteins (both for

SynCon and native). Each peptide pool was composed of 32 peptides (total of 96 peptides per protein).

ELISA

We coated NUNC MaxiSorp 96-well plates (Thermo Scientific) with 1 µg/mL murine Fshr extracellular domain (GenScript) in PBS overnight at 4°C. We washed the plates with PBS-0.5% Tween20 and blocked with PBS-10% fetal bovine serum (FBS) for 1 hr at room temperature. We incubated with the indicated dilutions of mouse sera for 2 hr at 37°C and followed with Goat Anti-Mouse horseradish peroxidase (HRP) (IgG H&L) (Abcam, ab6789) for 1 hr at room temperature. We developed HRP using SIGMAFAST OPD (Sigma).

Immunoblotting

Protein extraction, denaturation, and western blotting were performed as previously described.³⁷ Membranes were blotted with anti-FSHR (ab75200, Abcam) and anti- β -actin (a5441, Sigma-Aldrich). Images were captured with ImageQuantLAS 4000 (GE Healthcare Life Sciences).

T Cell Expansion and Activation

We harvested splenocytes from vaccinated mice and pulsed them with 10 µg/mL FSHR peptides and 30 UI/mL IL-2. We refreshed the peptides and IL-2 (PeproTech) with irradiated (4,000 rad) splenocytes from naive mice (1:3–10 T cell:splenocyte ratio) once a week. At 4–6 weeks after initiating the T cell expansion, we negatively selected the living cells using the dead cell removal kit (EasySep), which consisted of CD8⁺ T cells, and we injected 2 million intraperitoneally into tumor-bearing mice. Alternatively, we sorted CD3⁺CD8⁺7-AAD T cells. As a control for the adoptive T cell transfer, we isolated CD8 T cells from the spleens of naive mice and expanded them using anti-CD3- anti-CD28-coupled magnetic beads (Invitrogen) and IL-2 (30 IU/mL). At 5 days after initiating the T cell expansion, we removed the beads and used them for the adoptive T cell transfer.

In Vitro Cytotoxicity

We plated 5,000 ID8-*Defb29/Vegf-a* or ID8-*Defb29/Vegf-a-Fshr* cells per well in a 96-well plate, and, 18 hr later, we coincubated them for 5 hr with 5–50,000 T cells expanded with the appropriate peptide. We performed a flow cytometry-based assay as reported previously.⁹ Briefly, after 5 hr, we collected the supernatant; washed the wells with PBS; trypsinized the cells; and stained them with anti-mouse CD45, Annexin V (BioLegend), and 7-AAD (Thermo Fisher Scientific).

Immunofluorescence

200,000 293T cells were transfected with 2 µg murine FSHR, FSHR consensus DNA vaccine, or pVAX empty vector using Lipofectamine 2000, according to the manufacturer's instructions, on poly-L-lysine cover slides in 6-well plates. 48 hr later, cells were washed with PBS, fixed with 4% paraformaldehyde, permeabilized with Triton X-100 0.5% in PBS, and stained with sera derived from polyclonal anti-mouse FSHR antibodies obtained from mice immunized with native FSHR DNA followed by Alexa Fluor 488-conjugated secondary anti-mouse IgG antibodies (Invitrogen).

Slides were viewed using a Leica TCS SP5 Confocal Laser Scanning Microscope and the LAS AF software (Leica).

Statistical Analysis

Differences between the means of experimental groups were calculated using a two-tailed unpaired Student's *t* test. Comparisons between more than one group were made with one-way ANOVA or Kruskal-Wallis in case of nonparametric distribution. Error bars represent SEM. Survival rates were compared using the log-rank test. All statistical analyses were done using Graph Pad Prism 7.0. *p* < 0.05 was considered statistically significant.

SUPPLEMENTAL INFORMATION

Supplemental Information includes six figures and Supplemental Materials and Methods and can be found with this article online at <https://doi.org/10.1016/j.jymthe.2018.11.014>.

AUTHOR CONTRIBUTIONS

Conceptualization, A.P.-P., J.Y., and D.B.W.; Methodology, A.P.-P. and E.K.D.; Investigation, A.P.-P., K.W., and X.Y.; Writing – Original Draft, A.P.-P.; Writing – Review & Editing, A.P.-P. and D.B.W.; Funding Acquisition, D.B.W. and L.J.M.; Resources, D.B.W., J.Y., L.J.M., and K.M.; Supervision, D.B.W. and L.J.M.

CONFLICTS OF INTEREST

D.B.W. receives a commercial research grant from Inovio Pharmaceuticals; has received speakers bureau honoraria from Inovio Pharmaceuticals, GeneOne, and AstraZeneca; has an ownership interest (including patents) in Inovio Pharmaceuticals; and is a consultant/advisory board member for Inovio Pharmaceuticals. J.Y. and A.M.S. are employees at Inovio Pharmaceuticals. The other authors declare no conflicts of interests. J.Y., A.P.-P., and D.B.W. hold a provisional patent for the FSHR DNA vaccine.

ACKNOWLEDGMENTS

We want to thank the NIH Tetramer Core for the generation of the H2-K(b)-STYRLKKL tetramer. This work was supported by a Penn/Wistar Institute NIH SPORE (P50CA174523 to D.B.W.), the Wistar National Cancer Institute Cancer Center (P30 CA010815), the W.W. Smith Family Trust (to D.B.W.), funding from the Basser Foundation (to D.B.W.), and a grant from Inovio Pharmaceuticals (to D.B.W.). E.K.D. was supported by F32 CA213795. We would like to thank the Wistar Flow Cytometry Facility and Animal Facility for their technical assistance.

REFERENCES

1. Siegel, R.L., Miller, K.D., and Jemal, A. (2016). Cancer statistics, 2016. *CA Cancer J. Clin.* 66, 7–30.
2. Chiva, L., Lapuente, F., Castellanos, T., Alonso, S., and Gonzalez-Martin, A. (2016). What Should We Expect After a Complete Cytoreduction at the Time of Interval or Primary Debulking Surgery in Advanced Ovarian Cancer? *Ann. Surg. Oncol.* 23, 1666–1673.
3. Zhang, L., Conejo-Garcia, J.R., Katsaros, D., Gimotty, P.A., Massobrio, M., Regnani, G., Makrigiannakis, A., Gray, H., Schlienger, K., Liebman, M.N., et al. (2003). Intratumoral T cells, recurrence, and survival in epithelial ovarian cancer. *N. Engl. J. Med.* 348, 203–213.
4. Stumpf, M., Hasenburger, A., Riener, M.O., Jütting, U., Wang, C., Shen, Y., Orłowska-Volk, M., Fisch, P., Wang, Z., Gitsch, G., et al. (2009). Intraepithelial CD8-positive T lymphocytes predict survival for patients with serous stage III ovarian carcinomas: relevance of clonal selection of T lymphocytes. *Br. J. Cancer* 101, 1513–1521.
5. Coukos, G., Tanyi, J., and Kandalaf, L.E. (2016). Opportunities in immunotherapy of ovarian cancer. *Ann. Oncol.* 27 (Suppl 1), i11–i15.
6. Radu, A., Pichon, C., Camparo, P., Antoine, M., Allory, Y., Couvelard, A., Fromont, G., Hai, M.T., and Ghinea, N. (2010). Expression of follicle-stimulating hormone receptor in tumor blood vessels. *N. Engl. J. Med.* 363, 1621–1630.
7. Siraj, A., Desestret, V., Antoine, M., Fromont, G., Huerre, M., Sanson, M., Camparo, P., Pichon, C., Planeix, F., Gonin, J., et al. (2013). Expression of follicle-stimulating hormone receptor by the vascular endothelium in tumor metastases. *BMC Cancer* 13, 246.
8. Mariani, S., Salvatori, L., Basciani, S., Arizzi, M., Franco, G., Petrangeli, E., Spera, G., and Gnassi, L. (2006). Expression and cellular localization of follicle-stimulating hormone receptor in normal human prostate, benign prostatic hyperplasia and prostate cancer. *J. Urol.* 175, 2072–2077, discussion 2077.
9. Perales-Puchalt, A., Svoronos, N., Rutkowski, M.R., Allegrezza, M.J., Tesone, A.J., Payne, K.K., Wickramasinghe, J., Nguyen, J.M., O'Brien, S.W., Gumireddy, K., et al. (2017). Follicle-Stimulating Hormone Receptor Is Expressed by Most Ovarian Cancer Subtypes and Is a Safe and Effective Immunotherapeutic Target. *Clin. Cancer Res.* 23, 441–453.
10. Bagarazzi, M.L., Yan, J., Morrow, M.P., Shen, X., Parker, R.L., Lee, J.C., Giffear, M., Pankhong, P., Khan, A.S., Broderick, K.E., et al. (2012). Immunotherapy against HPV16/18 generates potent TH1 and cytotoxic cellular immune responses. *Sci. Transl. Med.* 4, 155ra138.
11. Kalams, S.A., Parker, S.D., Elizaga, M., Metch, B., Edupuganti, S., Hural, J., De Rosa, S., Carter, D.K., Rybczyk, K., Frank, I., et al.; NIAID HIV Vaccine Trials Network (2013). Safety and comparative immunogenicity of an HIV-1 DNA vaccine in combination with plasmid interleukin 12 and impact of intramuscular electroporation for delivery. *J. Infect. Dis.* 208, 818–829.
12. Morrow, M.P., Tebas, P., Yan, J., Ramirez, L., Slager, A., Kraynyak, K., Diehl, M., Shah, D., Khan, A., Lee, J., et al. (2015). Synthetic consensus HIV-1 DNA induces potent cellular immune responses and synthesis of granzyme B, perforin in HIV infected individuals. *Mol. Ther.* 23, 591–601.
13. Tebas, P., Roberts, C.C., Muthumani, K., Reuschel, E.L., Kudchodkar, S.B., Zaidi, F.I., White, S., Khan, A.S., Racine, T., Choi, H., et al. (2017). Safety and Immunogenicity of an Anti-Zika Virus DNA Vaccine - Preliminary Report. *N. Engl. J. Med.* Published online October 4, 2017. <https://doi.org/10.1056/NEJMoa1708120>.
14. Sardesai, N.Y., and Weiner, D.B. (2011). Electroporation delivery of DNA vaccines: prospects for success. *Curr. Opin. Immunol.* 23, 421–429.
15. Flingai, S., Czerwonko, M., Goodman, J., Kudchodkar, S.B., Muthumani, K., and Weiner, D.B. (2013). Synthetic DNA vaccines: improved vaccine potency by electroporation and co-delivered genetic adjuvants. *Front. Immunol.* 4, 354.
16. Duperret, E.K., Trautz, A., Ammons, D., Perales-Puchalt, A., Wise, M.C., Yan, J., Reed, C., and Weiner, D.B. (2018). Alteration of the Tumor Stroma Using a Consensus DNA Vaccine Targeting Fibroblast Activation Protein (FAP) Synergizes with Antitumor Vaccine Therapy in Mice. *Clin. Cancer Res.* 24, 1190–1201.
17. Walters, J.N., Ferraro, B., Duperret, E.K., Kraynyak, K.A., Chu, J., Saint-Fleur, A., Yan, J., Levitsky, H., Khan, A.S., Sardesai, N.Y., and Weiner, D.B. (2017). A Novel DNA Vaccine Platform Enhances Neo-antigen-like T Cell Responses against WT1 to Break Tolerance and Induce Anti-tumor Immunity. *Mol. Ther.* 25, 976–988.
18. Trimble, C.L., Morrow, M.P., Kraynyak, K.A., Shen, X., Dallas, M., Yan, J., Edwards, L., Parker, R.L., Denny, L., Giffear, M., et al. (2015). Safety, efficacy, and immunogenicity of VGX-3100, a therapeutic synthetic DNA vaccine targeting human papillomavirus 16 and 18 E6 and E7 proteins for cervical intraepithelial neoplasia 2/3: a randomised, double-blind, placebo-controlled phase 2b trial. *Lancet* 386, 2078–2088.
19. Svoronos, N., Perales-Puchalt, A., Allegrezza, M.J., Rutkowski, M.R., Payne, K.K., Tesone, A.J., Nguyen, J.M., Curiel, T.J., Cadungog, M.G., Singhal, S., et al. (2017). Tumor Cell-Independent Estrogen Signaling Drives Disease Progression through Mobilization of Myeloid-Derived Suppressor Cells. *Cancer Discov.* 7, 72–85.

20. Cubillos-Ruiz, J.R., Silberman, P.C., Rutkowski, M.R., Chopra, S., Perales-Puchalt, A., Song, M., Zhang, S., Bettigole, S.E., Gupta, D., Holcomb, K., et al. (2015). ER Stress Sensor XBP1 Controls Anti-tumor Immunity by Disrupting Dendritic Cell Homeostasis. *Cell* 161, 1527–1538.
21. Stephen, T.L., Rutkowski, M.R., Allegranza, M.J., Perales-Puchalt, A., Tesone, A.J., Svoronos, N., Nguyen, J.M., Sarmin, F., Borowsky, M.E., Tchou, J., and Conejo-Garcia, J.R. (2014). Transforming growth factor β -mediated suppression of anti-tumor T cells requires FoxP1 transcription factor expression. *Immunity* 41, 427–439.
22. Yang, J.S., Kim, J.J., Hwang, D., Choo, A.Y., Dang, K., Maguire, H., Kudchodkar, S., Ramanathan, M.P., and Weiner, D.B. (2001). Induction of potent Th1-type immune responses from a novel DNA vaccine for West Nile virus New York isolate (WNV-NY1999). *J. Infect. Dis.* 184, 809–816.
23. Pagès, F., Berger, A., Camus, M., Sanchez-Cabo, F., Costes, A., Molitor, R., Mecnik, B., Kirilovsky, A., Nilsson, M., Damotte, D., et al. (2005). Effector memory T cells, early metastasis, and survival in colorectal cancer. *N. Engl. J. Med.* 353, 2654–2666.
24. Urbanska, K., Stashwick, C., Poussin, M., and Powell, D.J., Jr. (2015). Follicle-Stimulating Hormone Receptor as a Target in the Redirected T-cell Therapy for Cancer. *Cancer Immunol. Res.* 3, 1130–1137.
25. Suzuki, S., Sakata, J., Utsumi, F., Sekiya, R., Kajiyama, H., Shibata, K., Kikkawa, F., and Nakatsura, T. (2016). Efficacy of glypican-3-derived peptide vaccine therapy on the survival of patients with refractory ovarian clear cell carcinoma. *Oncolimmunology* 5, e1238542.
26. Antonilli, M., Rahimi, H., Visconti, V., Napoletano, C., Ruscito, I., Zizzari, I.G., Caponnetto, S., Barchiesi, G., Iadarola, R., Pierelli, L., et al. (2016). Triple peptide vaccination as consolidation treatment in women affected by ovarian and breast cancer: Clinical and immunological data of a phase I/II clinical trial. *Int. J. Oncol.* 48, 1369–1378.
27. Rock, K.L., Reits, E., and Neefjes, J. (2016). Present Yourself! By MHC Class I and MHC Class II Molecules. *Trends Immunol.* 37, 724–737.
28. Kandalaf, L.E., Powell, D.J., Jr., Chiang, C.L., Tanyi, J., Kim, S., Bosch, M., Montone, K., Mick, R., Levine, B.L., Torigian, D.A., et al. (2013). Autologous lysate-pulsed dendritic cell vaccination followed by adoptive transfer of vaccine-primed ex vivo co-stimulated T cells in recurrent ovarian cancer. *Oncolimmunology* 2, e22664.
29. Chiang, C.L., Kandalaf, L.E., Tanyi, J., Hagemann, A.R., Motz, G.T., Svoronos, N., Montone, K., Mantia-Smaldone, G.M., Smith, L., Nisenbaum, H.L., et al. (2013). A dendritic cell vaccine pulsed with autologous hypochlorous acid-oxidized ovarian cancer lysate primes effective broad antitumor immunity: from bench to bedside. *Clin. Cancer Res.* 19, 4801–4815.
30. Preston, C.C., Goode, E.L., Hartmann, L.C., Kalli, K.R., and Knutson, K.L. (2011). Immunity and immune suppression in human ovarian cancer. *Immunotherapy* 3, 539–556.
31. Zhang, S., Ke, X., Zeng, S., Wu, M., Lou, J., Wu, L., Huang, P., Huang, L., Wang, F., and Pan, S. (2015). Analysis of CD8⁺ Treg cells in patients with ovarian cancer: a possible mechanism for immune impairment. *Cell. Mol. Immunol.* 12, 580–591.
32. McGuire, W.P., Hoskins, W.J., Brady, M.F., Kucera, P.R., Partridge, E.E., Look, K.Y., Clarke-Pearson, D.L., and Davidson, M. (1996). Cyclophosphamide and cisplatin compared with paclitaxel and cisplatin in patients with stage III and stage IV ovarian cancer. *N. Engl. J. Med.* 334, 1–6.
33. Friedlander, M., GebSKI, V., Gibbs, E., Davies, L., Bloomfield, R., Hilpert, F., Wenzel, L.B., Eek, D., Rodrigues, M., Clamp, A., et al. (2018). Health-related quality of life and patient-centred outcomes with olaparib maintenance after chemotherapy in patients with platinum-sensitive, relapsed ovarian cancer and a BRCA1/2 mutation (SOLO2/ENGOT-Ov-21): a placebo-controlled, phase 3 randomised trial. *Lancet Oncol.* 19, 1126–1134.
34. Pujade-Lauraine, E., Ledermann, J.A., Selle, F., GebSKI, V., Penson, R.T., Oza, A.M., Korach, J., Huzarski, T., Poveda, A., Pignata, S., et al.; SOLO2/ENGOT-Ov21 investigators (2017). Olaparib tablets as maintenance therapy in patients with platinum-sensitive, relapsed ovarian cancer and a BRCA1/2 mutation (SOLO2/ENGOT-Ov21): a double-blind, randomised, placebo-controlled, phase 3 trial. *Lancet Oncol.* 18, 1274–1284.
35. Hutchinson, L. (2017). Targeted therapies: SOLO2 confirms olaparib maintenance in ovarian cancer. *Nat. Rev. Clin. Oncol.* 14, 586–587.
36. MacGregor, R.R., Boyer, J.D., Ugen, K.E., Tebas, P., Higgins, T.J., Baine, Y., Ciccarelli, R.B., Ginsberg, R.S., and Weiner, D.B. (2005). Plasmid vaccination of stable HIV-positive subjects on antiviral treatment results in enhanced CD8 T-cell immunity and increased control of viral “blips”. *Vaccine* 23, 2066–2073.
37. Tesone, A.J., Rutkowski, M.R., Brencicova, E., Svoronos, N., Perales-Puchalt, A., Stephen, T.L., Allegranza, M.J., Payne, K.K., Nguyen, J.M., Wickramasinghe, J., et al. (2016). Satb1 Overexpression Drives Tumor-Promoting Activities in Cancer-Associated Dendritic Cells. *Cell Rep.* 14, 1774–1786.

YMTHE, Volume 27

Supplemental Information

Engineered DNA Vaccination against

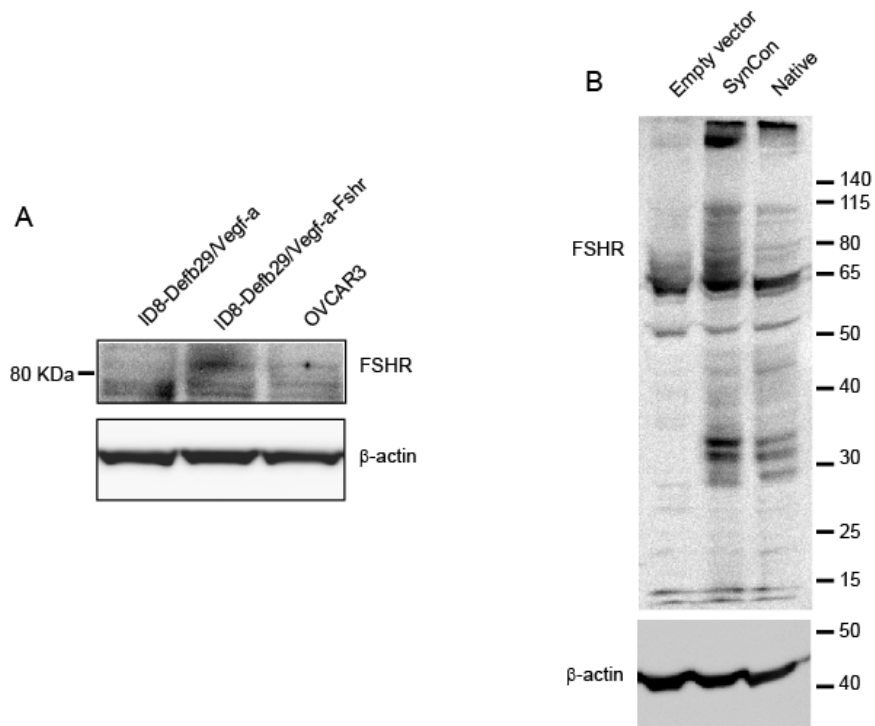
Follicle-Stimulating Hormone Receptor Delays

Ovarian Cancer Progression in Animal Models

Alfredo Perales-Puchalt, Krzysztof Wojtak, Elizabeth K. Duperret, Xue Yang, Anna M. Slager, Jian Yan, Kar Muthumani, Luis J. Montaner, and David B. Weiner

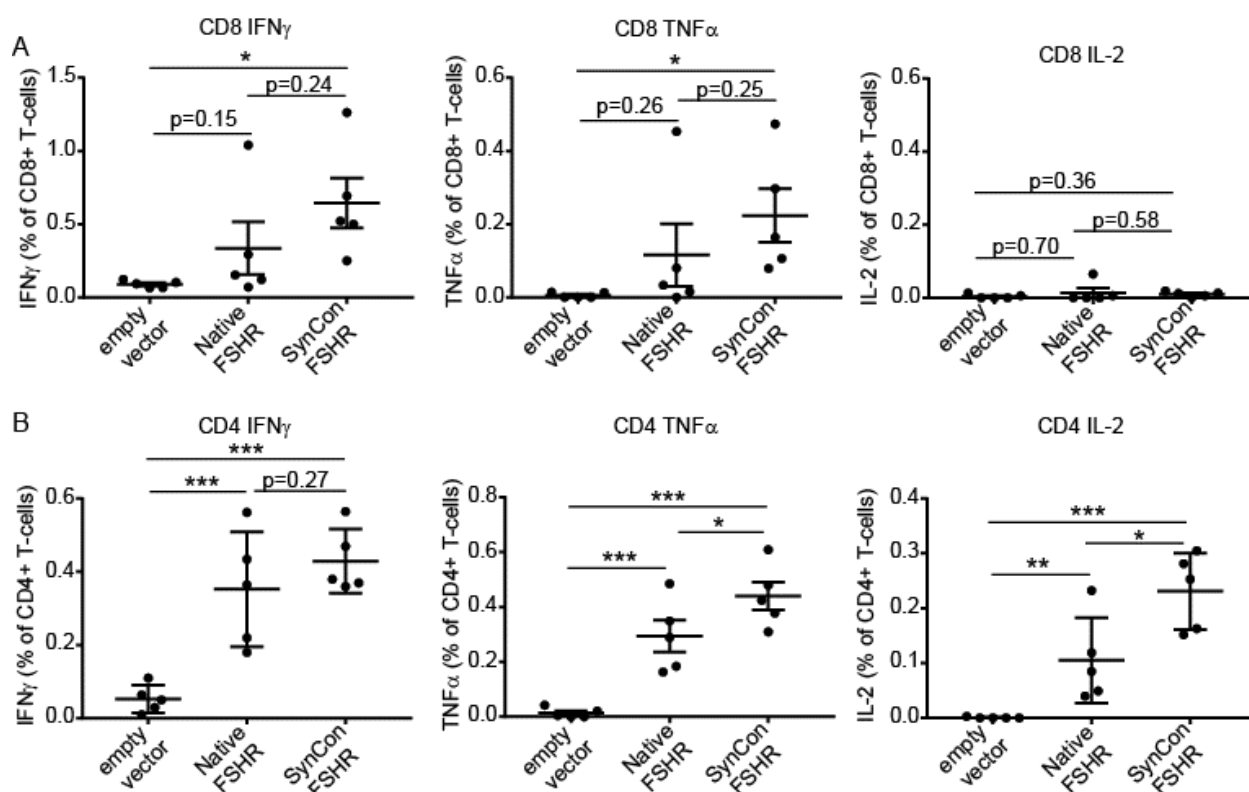
SUPPLEMENTAL FIGURES

SUPPLEMENTAL FIGURE 1



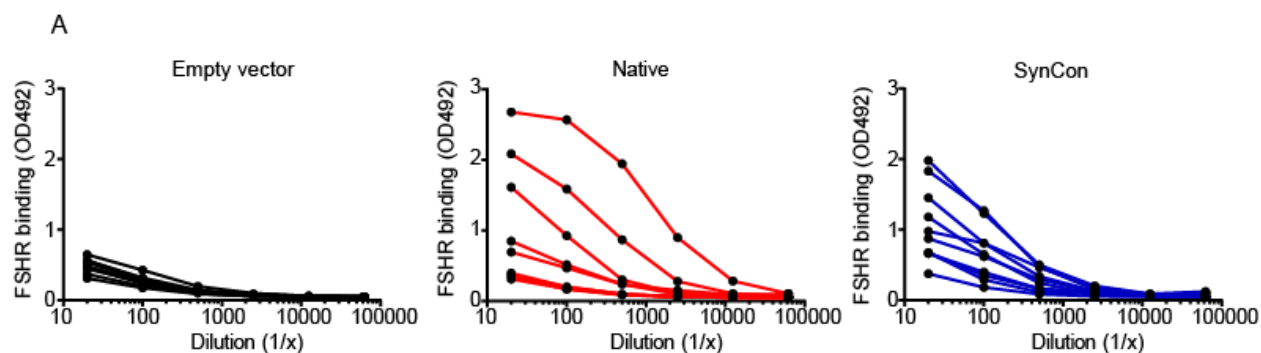
Supplemental Figure 1. Expression of SynCon and native FSHR vaccines. Western blot of protein derived from (A) OVCAR3, ID8-*Defb29/Vegf-a-Fshr* and ID8-*Defb29/Vegf-a* and (B) murine FSHR SynCon vaccine, murine native FSHR vaccine or empty vector transfected 293T cells (10% gel MOPS buffer) blotted for FSHR and β -actin (representative of 2 experiments)

SUPPLEMENTAL FIGURE 2



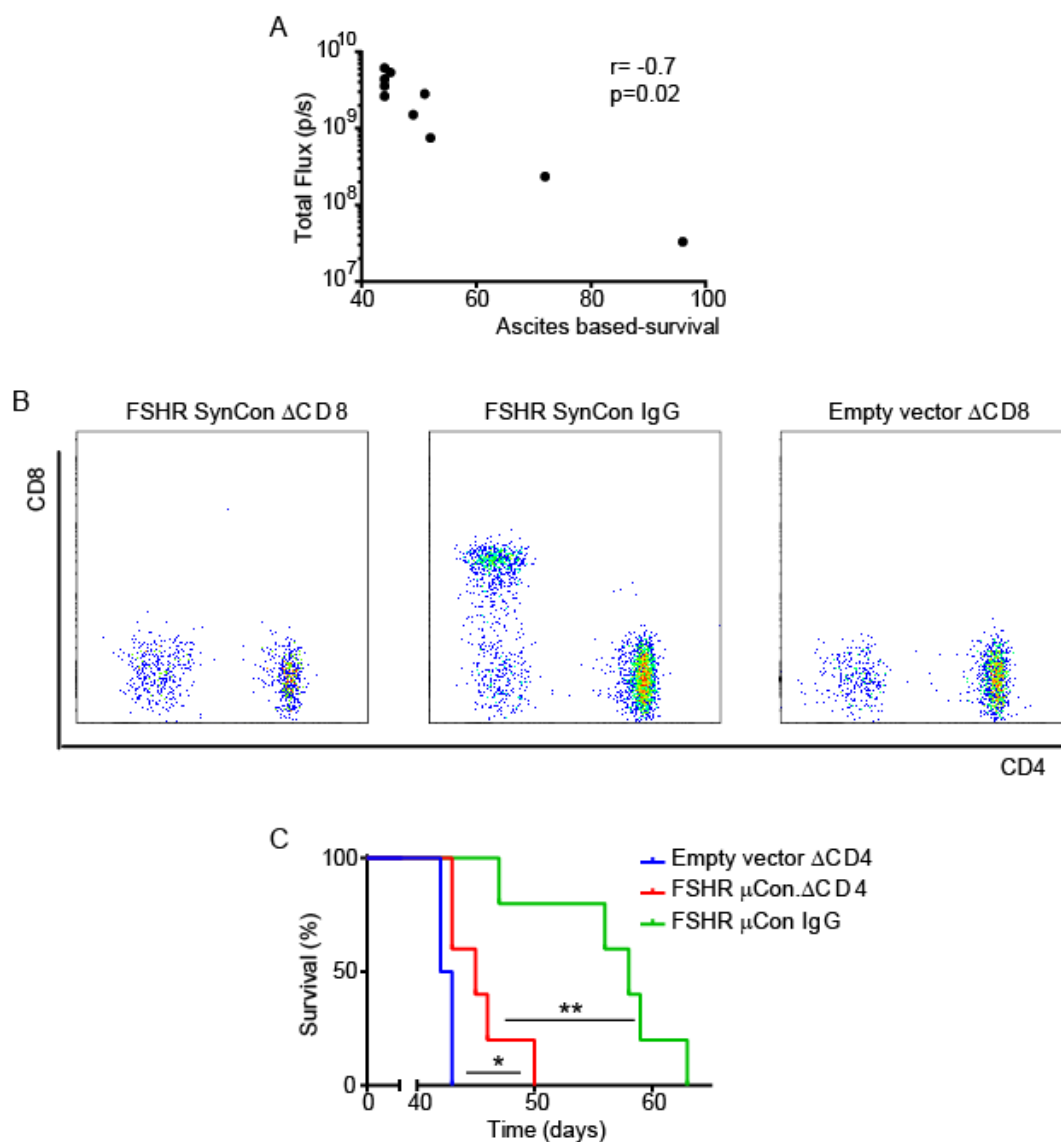
Supplemental Figure 2. Mouse FSHR DNA vaccine generates strong CD8 and CD4 responses when pulsed with vaccine matched peptides. Percentage of IFN γ , TNF α and IL-2 produced by (A) CD8+ or (B) CD4+ T cells from the spleen of mice immunized with FSHR SynCon vaccine, FSHR native vaccine or empty vector stimulated with consensus vaccine matched peptides. ANOVA. * $p < 0.05$, ** $p < 0.01$, *** $p < 0.001$.

SUPPLEMENTAL FIGURE 3



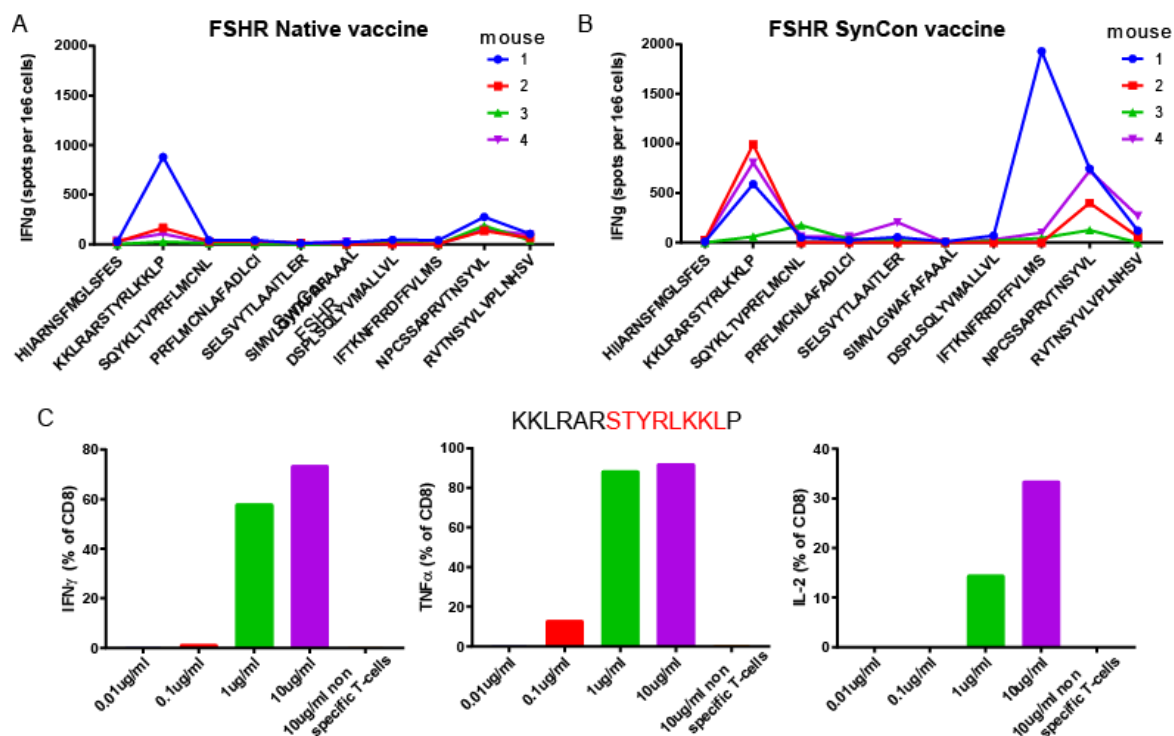
Supplemental Figure 3. Mouse FSHR DNA vaccine generates antibodies against FSHR. (A) Binding of sera from mice vaccinated with FSHR vaccine, native FSHR or pVAX empty vector to the extracellular domain of native murine FSHR in a binding ELISA. Each curve represents one mouse.

SUPPLEMENTAL FIGURE 4



Supplemental Figure 4. CD8 and CD8 depletion experiment. (A) Correlation between luciferase expression and ascites-based survival in luciferase transfected ID8-*Defb29/Vegf-a-Fshr* tumor challenge. (B) We vaccinated mice and challenged with ID8-*Defb29/Vegf-a-Fshr* one week after the last immunization. One day prior to the tumor challenge and twice weekly thereafter we administered either anti-mouse CD8 or rat polyclonal IgG. Flow plots showing CD4⁺ and CD8⁺ T cells in the tumor microenvironment of the different groups at day 21 after tumor inoculation. (C) Survival plot of the FSHR SynCon vaccine or pVAX empty vector with or without CD8 depletion (n=5 mice per group). Pearson correlation, Log-rank. *p<0.05, **p<0.01

SUPPLEMENTAL FIGURE 5



Supplemental Figure 5. Murine FSHR SynCon vaccine increases the number and intensity of immunogenic sequences of FSHR. (A&B) IFN γ ELISpot of splenocytes from mice immunized with murine FSHR SynCon vaccine, native FSHR vaccine or empty vector pulsed with FSHR derived peptides predicted to bind with high affinity to H2-K(b) or H2-D (b) (n=4 mice per group). (C) Percentage of IFN γ , TNF α and IL-2 produced by CD8⁺ T cells expanded from mice immunized with murine FSHR SynCon vaccine expanded with KKLRARSTYRLKCLP peptides and stimulated with the same peptides at different doses.

SUPPLEMENTAL FIGURE 6

A IEDB Analysis Resource

Home Help Example Reference Download Contact

MHC-I Binding Prediction Results

Input Sequences

#	Name	Sequence
1	sp P35378 FSHR_MOUSE Follicle-stimulating hormone receptor DE=Mus musculus CX-10090 GN=Fshr FE-2 SV-2	MALLLVSLAFLGSGSGCHHLLCHSNRVFLCODSKVTEIPDLPRIVAIE LRFVLTSLRVIPKGFSGCTDLEKICISQNDVLCVICADVSNLPNLIICI RIEKANNLLYINPEAFQNLPSLRVLLISATGIRKLPAPFKIQSLQKVLLD IQDRIINIHIIARNSFMGLSFESVILWLNKNGIQEIHCAFNGTQLDELNL SDRNIIFFI PNDVFGAGSGPVAIIPFRTKVVYSPIHKKI RARSTY RLKXKLSLDKFWLIEASLTVPSHCCAFANIRQTSLELHPICIKSIESRD IDDMTPGDDQFVSLVDDEPVSYGSGDMLYSEGDYDLNCIFVDVTCSPK AFNPCCDINGVILRVLIWFSILAITGNTTVLWLTTSQYKLTVPRLAI CNLAFADLCIGIYLLIASVDIHTKSQVHYAIDMQTGAGCDAAGFFTVF ASFI SVYTI AATTI FRMHTTTHAQI FCKVQI CHAASTPM GWAFAPAAA LFPZFGISSYNYKYSICLPNDIDSPLSOLYVWLLVNLALAFVVICGCTH IYLTVRNPNIVSSRDTKIAKRWATLITDGLMAPILFTAISAGLVPL ITVSKKILLVLFYFINSCLMPFLVIFTKFRDRDFVLSKFGCYEVQA QIVKTESSITHNFHFRKNPCSSAPRVTSVWLVPLNHSVQN

Prediction method: IEDB recommended | Low percentile_rank = good binders

Download result

Citations

Check to expand the result:

Allele	#	Start	End	Length	Peptide	Method used	Percentile_rank	ANN IC50(nM)	ANN rank	SMM IC50(nM)	SMM rank
H-2-Kb	1	455	462	8	SVYTLAAI	Consensus (ann/smm)	0.3	11.70	0.2	75.24	0.4
H-2-Kb	1	401	408	8	CNLAFADL	Consensus (ann/smm)	0.25	24.33	0.2	48.75	0.3
H-2-Kb	1	679	686	8	NSYVLVPL	Consensus (ann/smm)	0.3	32.62	0.3	53.30	0.3
H-2-Kb	1	248	255	8	STYRLKKL	Consensus (ann/smm)	0.35	35.52	0.3	68.35	0.4
H-2-Kb	1	527	534	8	QIYVPAI I	Consensus (ann/smm)	0.55	72.50	0.3	174.46	0.6

B IEDB Analysis Resource

Home Help Example Reference Download Contact

MHC-I Processing Prediction Results

Input Sequences

#	Name	Sequence
1	sp P35378 FSHR_MOUSE Follicle-stimulating hormone receptor DE=Mus musculus CX-10090 GN=Fshr FE-2 SV-2	MALLLVSLAFLGSGSGCHHLLCHSNRVFLCODSKVTEIPDLPRIVAIE LRFVLTSLRVIPKGFSGCTDLEKICISQNDVLCVICADVSNLPNLIICI RIEKANNLLYINPEAFQNLPSLRVLLISATGIRKLPAPFKIQSLQKVLLD IQDRIINIHIIARNSFMGLSFESVILWLNKNGIQEIHCAFNGTQLDELNL SDRNIIFFI PNDVFGAGSGPVAIIPFRTKVVYSPIHKKI RARSTY RLKXKLSLDKFWLIEASLTVPSHCCAFANIRQTSLELHPICIKSIESRD IDDMTPGDDQFVSLVDDEPVSYGSGDMLYSEGDYDLNCIFVDVTCSPK AFNPCCDINGVILRVLIWFSILAITGNTTVLWLTTSQYKLTVPRLAI CNLAFADLCIGIYLLIASVDIHTKSQVHYAIDMQTGAGCDAAGFFTVF ASFI SVYTI AATTI FRMHTTTHAQI FCKVQI CHAASTPM GWAFAPAAA LFPZFGISSYNYKYSICLPNDIDSPLSOLYVWLLVNLALAFVVICGCTH IYLTVRNPNIVSSRDTKIAKRWATLITDGLMAPILFTAISAGLVPL ITVSKKILLVLFYFINSCLMPFLVIFTKFRDRDFVLSKFGCYEVQA QIVKTESSITHNFHFRKNPCSSAPRVTSVWLVPLNHSVQN

Prediction method: recommended | High Score = high efficiency

Download result

Citations

Allele	#	Start	End	Peptide Length	Peptide	Proteasome Score	TAP Score	MHC Score	Processing Score	Total Score	MHC IC50[nM]
H-2-Kb	1	488	501	14	LVNLGMNFAAVIL	1.39	0.54	-1.21	1.93	0.72	18.2
H-2-Kb	1	490	501	12	VLGMVFAVAL	1.39	0.40	-1.21	1.79	0.56	18.2
H-2-Kb	1	493	501	9	WAFAPDAL	1.39	0.46	-1.58	1.85	0.50	22.7
H-2-Kb	1	490	502	13	VLGMVFAAALF	1.20	1.08	-1.81	2.26	0.47	84.6
H-2-Kb	1	489	501	13	MVLGMVFAAAL	1.39	0.51	-1.45	1.90	0.44	26.5
H-2-Kb	1	248	255	8	STYRLKKL	1.52	0.57	-1.06	2.08	0.42	45.7
H-2-Kb	1	100	100	9	TARNFPRGI	1.47	0.47	-1.05	1.94	0.25	44.9

Supplemental Figure 6. STYRLKKL is an FSHR derived octamer predicted to be efficiently processed and bind H2-K(b) with high affinity. (A) Screenshot showing the binding prediction to MCH-I of 8-mers derived from murine FSHR to H2-K(b) and H2-D(b) using the immunopeptide database (<http://tools.iedb.org/mhci/>). (B) Screenshot showing the proteasome and TAP processing prediction of all potential FSHR-derived peptides and binding to H2-K(b) and H2-D(b) using the immunopeptide database (<http://tools.iedb.org/processing/>).

SUPPLEMENTAL METHODS**Mouse SynCon FSHR DNA sequence**

ATGGA CTGGACCTGGATTCTGTT CCTGGTGGCCGCTGCCACAAGGGTGC ACTCCTGC
CACC ACTGGCTGTGCCACTGTTCTAACAGGGTGTTCCTGTGCCAGGACAGCAAGGTG
ACCGAGATCCCTCCCGATCTGCCCCGGAACGCCATCGAGCTGCGCTTCGTGCTGACA
AAGCTGAGAGTGATCCCTAAGGGCTCCTTCTCTGGCTTTGGAGATCTGGAGAAGATC
GAGATCTCCAGAACGACGTGCTGGAAGTGATCGAGGCCGACGTGTT CAGCAACCT
GCCTAAGCTGCACGAGATCCGGATCGAGAAGGCCAACACCTGCTGTACATCAACC
CCGAGGCTTTCCAGAACCTGCCTAGCCTGCGCTACCTGCTGATCTCCAACACCGGCA
TCAAGCACCTGCCAGCCGTGCACAAGATCCAGAGCCTGCAGAAGGTGCTGCTGGAC
ATCCAGGATAACATCAACATCCACATCATCGCTAGAACTCCTTCATGGGACTGTCT
TTTGAGAGCGTGATCCTGTGGCTGAACAAGAACGGCATCCAGGAGATCCACA ACTG
TGCCTTTAACGGAACACAGCTGGACGAGCTGAACCTGTCTGATAACAACAACCTGG
AGGAGCTGCCTAACGACGTGTTCCAGGGCGCCAGCGGACCAGTGATCCTGGATATC
TCCAGGACCAAGGTGCACTCTCTGCCCAACCACGGCCTGGAGAACCTGAAGAAGCT
GAGGGCCAGATCCACATA CAGACTGAAGAAGCTGCCTTCTCTGGACAAGTTCGTGA
CCCTGATGGAGGCTTCTCTGACATAACCAAGCCACTGCTGTGCCTTTGCTAACTGGA
GGAGACAGATCAGCGAGCTGCACCCAATCTGTAACAAGTCCATCCTGCGGCAGGAC
ATCGACGATATGACCCAGATCGGAGATCAGCGCGTGAGCCTGATCGACGATGAGCC
CTCCTACGGCAAGGGATCTGACATGATGTACAGCGAGTTCGACTTTGATCTGTGCAA
CGAGGTGGTGGATGTGACATGTTCCCAAAGCCCGACGCCTTCAACCCCTGCGAGG
ATATCATGGGCTACAACATCCTGCGGGTGCTGATCTGGTTTATCTCCATCCTGGCTAT
CACCGGAAACACCACAGTGCTGGTGGTGGCTGACCACATCTCAGTACAAGCTGACAG
TGCTCGCTTCCTGATGTGCAACCTGGCCTTTGCTGACCTGTGCATCGGCATCTACCT
GCTGCTGATCGCCTCTGTGGATATCCACACCAAGAGCCAGTACCACA ACTACGCCAT
CGACTGGCAGACCGGCGCTGGATGTGATGCTGCCGGATTCTTTACAGTGTTGCGCTC
CGAGCTGAGCGTGTAACCCCTGACAGCTATCACCCCTGGCCAGGGCTCACACCATCAC
ACACGCCATGCAGCTGGAGTGCAAGGTGCAGCTGAGACACGCTGCCTCTATCATGG
TGCTGGGCTGGACATTCGCTTTTGCTGCCGCTCTGTTCCCAATCTTTGGAATCAGCTC
CTACATGAAGGTGTCCATCTGTCTGCCTATGGACATCGATAGCCCACTGTCCCAGCT
GTACGTGATGGCCCTGCTGGTGGTGAACGTGCTGGCCTTCGTGGTCATCTGCGGCTG
TTACACCCACATCTACCTGACAGTGCGGAACCCCAACATCGTGTCTAGCTCCTCTGA
CACCAAGATCGCCAAGCGCATGGCTACCCTGATCTTCACAGATTTTCTGTGCATGGC
CCCAATCAGCTTCTTTGCCATCAGCGCCTCCCTGAAGGTGCCCTGATCACCGTGAG
CAAGGCTAAGATCCTGCTGGTGGTGTCTTCTACCCAATCAACTCCTGCGCCAACCCCTT
TCTGTACGCTATCTTCACAAAGAACTTTCGGCGCGACTTCTTTATCCTGATGAGCAA
GTTCCGGATGTTACGAGATGCAGGCCAGATCTACCGGACCGAGACAAGCTCCGCCA
CCCACA ACTTTCACGCTAGGAAGTCCC ACTGCAGCAGCGCCCCCAGGGTGACAAAC
TCTTACGTGCTGGTGCCTCTGAACCACAGCGTG CAGA ACTGATAA